

Supplemental Materials

Molecular Biology of the Cell

Furuta et al.

Legends for Supplemental Figures

Supplemental Figure S1 Establishment of the TET-based RCC1-conditional knockout cell line.

- (A) Diagram of the RCC1 locus and the gene targeted construct. B: BgIII and E: EcoRV sites. The position of the probes used for Southern hybridization and the expected size of each fragment used for hybridization are indicated.
- (B) Southern blot analysis of wild-type (Cl18: RCC1 +/+), heterozygote (First KO: RCC1 +/-), heterozygote + TRE promoter RCC1 (pUHD: RCC1 +/-, RCC1^{tTA}) and RCC1-null clone + TRE promoter RCC1 (2nd KO: RCC1 -/-, RCC1^{tTA}). Genomic DNA digested with BgIII or EcoRV was subjected to 1% agarose gel electrophoresis and hybridized with the L or R probe as shown in (A).
- (C) Protein levels of RCC1 in TET-based RCC1-conditional knockout cells following addition of TET. Whole cell lysates from wild type (Cl18) and TET-based RCC1 conditional knockout cells (RCC1 -/-, RCC1^{tTA}) at the indicated times after addition of 2 µg/ml TET were subjected to 5-20% SDS-PAGE, western blotting, and probed with affinity-purified polyclonal anti-RCC1 antibody. Loading control was probed with anti-histone H3.
- (D) Proliferation of TET-based RCC1 conditional knockout cells (RCC1 -/-, RCC1^{tTA}) after addition of TET. After addition of 2 µg/ml TET, live cells were counted after Trypan blue staining at the indicated times.
- (E) Cell cycle distribution of TET-based RCC1 conditional knockout cells (RCC1 -/-, RCC1^{tTA}) after addition of TET. Samples were collected at the indicated times after addition of 2 µg/ml TET. Propidium Iodide (x axis, linear scale) and BrdU (y axis, log scale) incorporation were analyzed by FACS. The boxes represent populations of G1 phase cells, and the numbers indicates the percentages of G1 populations.

Supplemental Figure S2

Sequence alignment of RCC1 from various species (*Gallus gallus*, *Homo sapiens*, and *Xenopus laevis*). Bold letters indicate expected NLS, and the box indicates the deleted region of NTD. Mutated residues are marked with arrowheads.

Supplemental Figure S3

Supporting data for Figure 3B. Subcellular localization of each RCC1 mutant in large field images. RCC1-deficient cells expressing RCC1^{wild}-GFP, RCC1^{Histone/DNA}-GFP, RCC1^{Δ20}-GFP or RCC1^{Ran}-GFP (green) were stained with Hoechst (blue), respectively. Scale bar, 10 μm.

Supplemental Figure S4

Supporting data for Figure 5A. Subcellular localization of each RCC mutant in large field images. RCC1-deficient cells expressing RCC1^{Δ20/histone/DNA} or RCC1^{Δ20/histone/DNA}-NLS (green) were stained with Hoechst (blue), respectively. Scale bar, 10 μm.

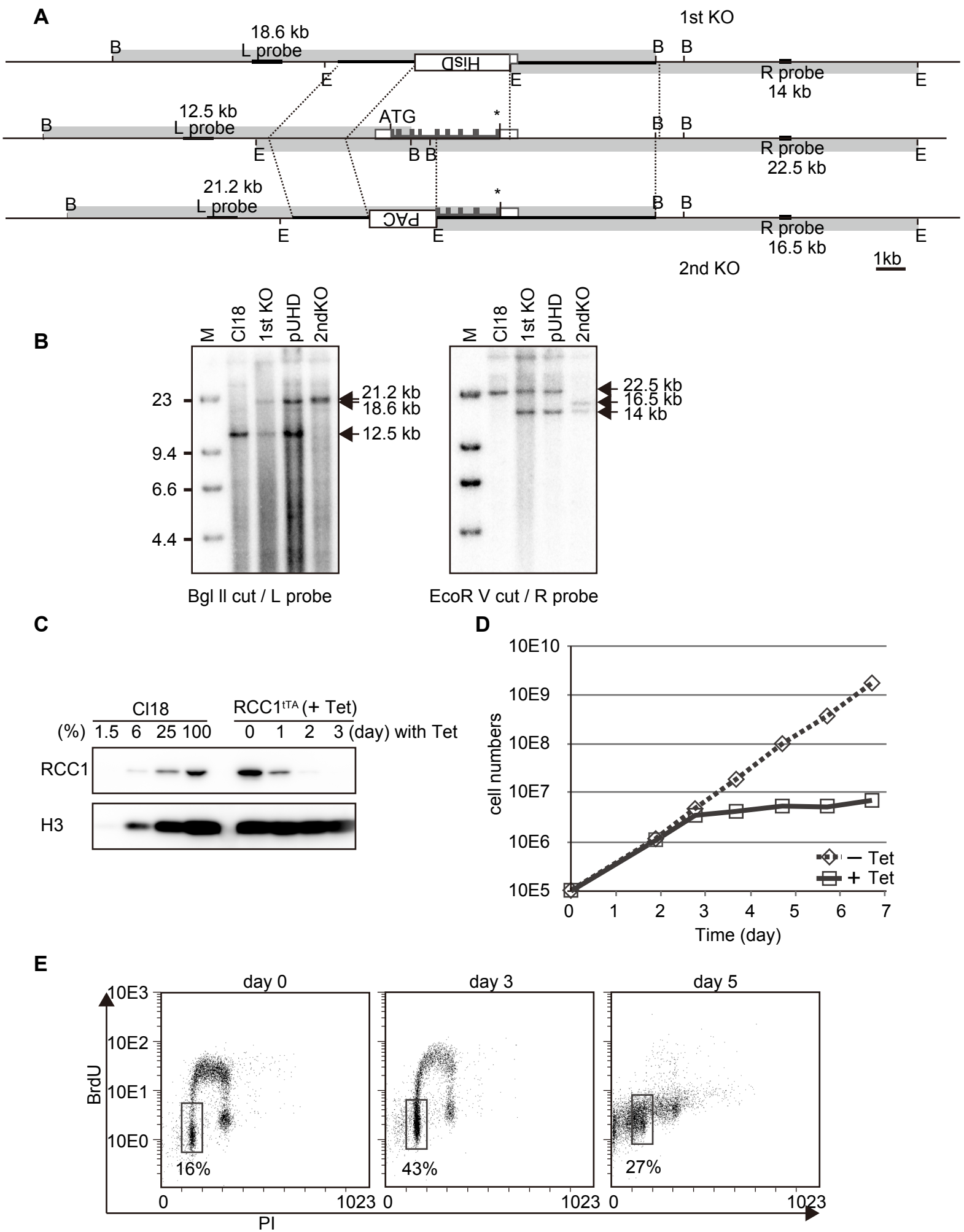
Supplemental Figure S5

Summary of phenotypes of RCC-deficient cells expressing various RCC mutants used in this paper. Ran GEF activity was predicted by cellular viability and its crystal structure study.

Supplemental Movies

Movie S1 Live cell imaging of Aid-based RCC1 conditional knockout cells (RCC1 -/-, RCC1^{tTA}, Aid-RCC1) expressing histone H2B-RFP (red) and GFP-tubulin (green). Cells were maintained in the presence of 2 μg/ml TET, and fluorescence images were acquired at 3-min intervals in the presence of 500 μM IAA.

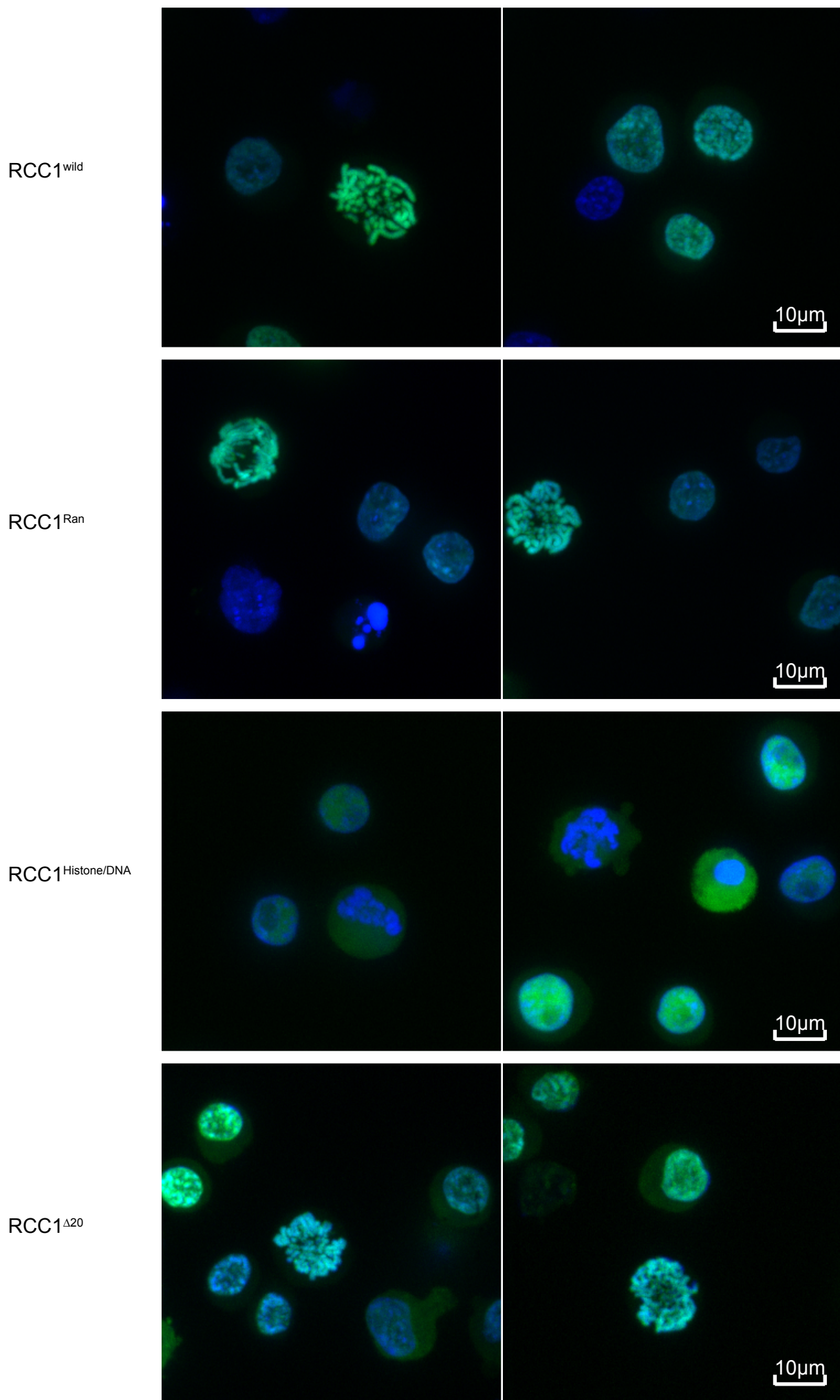
Movie S2 Live cell imaging of Aid-based RCC1 conditional knockout cells (RCC1 -/-, RCC1^{tTA}, Aid-RCC1) in the absence of IAA. This image is control for Movie S1.



Supplemental figure 1

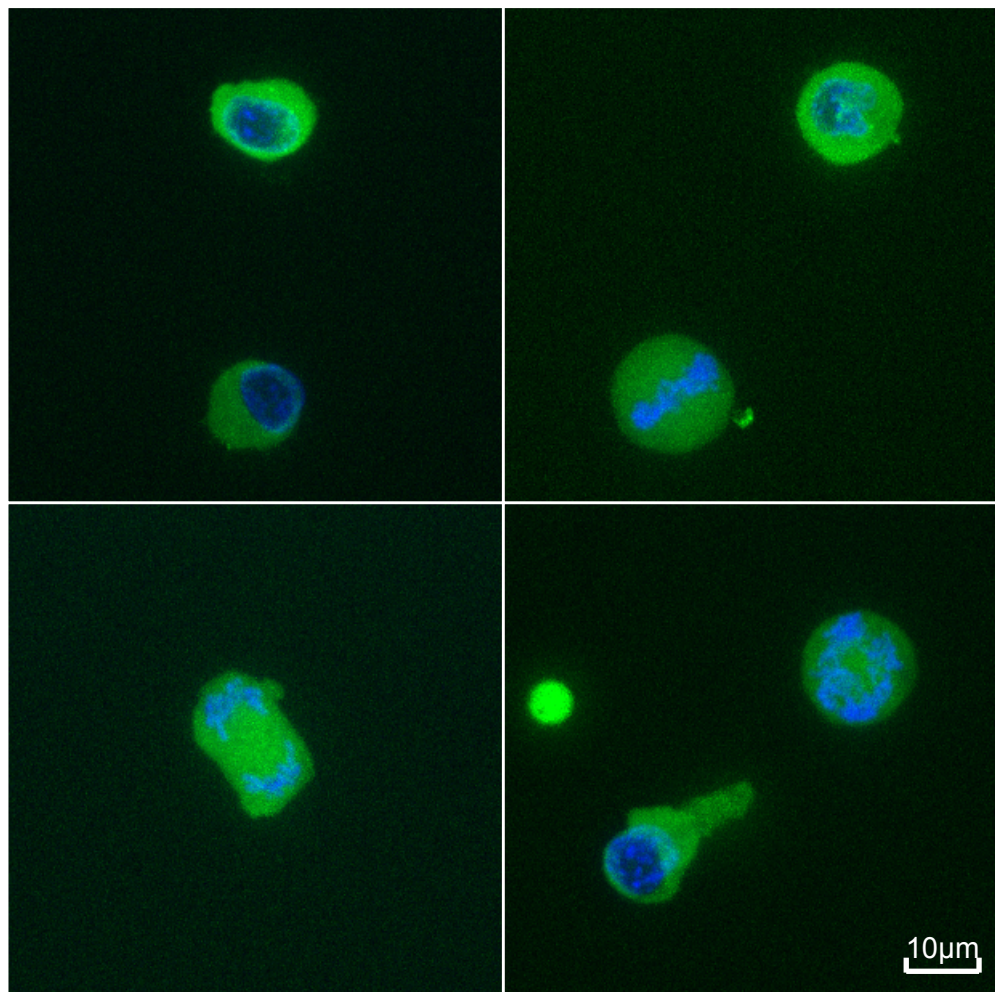
ggRCC1	MSGKRAAKK-SPALEE--PPEKKLK---VSHPSHRTQPGVLVLGQGDVGQLGLGQDV		
hRCC1	MSPKRIAKRRSPPADA--IPKSKKVK---VSHRSHSTE PGLVLTGQGDVGQLGLGENV		
x1RCC1	MKGKKTLKRTIAAEEESNGTSDVKKTKALPIVTHPSHGTVGQQVLTGQGDVGQLGLGEDI		
	* . * : * : . . : . . * * * * : * : * * * * * * * . * * * * * * * * * :		
	M76R		
ggRCC1	MERKKPALVQLPELMVQVEAGGMHTVCLSETGKIYTFCNDEALGRDTSEEGSECTPGP		
hRCC1	MERKKPALVSIPEDVVQAEAGGMHTVCLSKSGQVYSGCNCDEALGRDTSVEGSEMVPKG		
x1RCC1	MERKKPALVTLTEDIVQAAAGGMHTVCLGASGSIYTFCNDEALGRDTSEEGSEMOPGK		
	* * * * * * * * : * . * * * * * * * * . : * . * : * * * * * * * * * * * * * * :		
ggRCC1	VELQERVVQVSAGDSHTAALTDDGRVFIWGSFRDNNGVIGLLEPMKKSTPVVLLQLNVPV		
hRCC1	VELQEKKVQVSAGDSHTAALTDDGRVFLWGSFRDNNGVIGLLEPMKKSMVPVQVQLDVPV		
x1RCC1	VELAEKVVQVSAGDSHTAALTDEDGRVFVFGSFRDNNGVIGLLEPMKKSMVPVQVQINTPV		
	* * * * : * * * * * * * * : * * * * : * :		
	R216E	R231E	K233E
ggRCC1	VKIVSGNDHLVMLTVGDILFTCGCGEQGQLGRVPALFSNRGGRKGLQRLLVPQRVPVRGK		
hRCC1	VKVASGNDHLVMLTADGDLYTLCGCGEQGQLGRVPELFANRGGRQGLERLLVPKCVMLKSR		
x1RCC1	IKIASGNDHLVLLTVGDILYTSGCGEQGQLGRVPERFTNRGGRKGLERLLVPQCIHLKAK		
	: * : . * * * * : * . * * * : * :		
ggRCC1	GK---MRFQDAFCGAYFTFAITREGHIYGFGLSNYHQLGTQGTEPCFSQNLTSFKNSTK		
hRCC1	GSRGHVRFQDAFCGAYFTFAISHEGHVYGFGLSNYHQLGTPGTESCFIPQNLTSFKNSTK		
x1RCC1	GS-GRVHFQDVFCGAYFTFAVSQEGHVYGFGLSNYHQLGKNTQACYAPQNLTSFKNSTK		
	* . : * * * . * * * * * * * * : * : * * : * :		
ggRCC1	SWVGFSGGQHHTVCVDSEGKAYSLGRAEYGRLGLGE GAEEKSTPTVIPDLPSISSVACGA		
hRCC1	SWVGFSGGQHHTVCMDSEGKAYSLGRAEYGRLGLGE GAEEKSIPTLISRLPAVSSVACGA		
x1RCC1	SWIGFSGGQHHTVCVDSEGKAYSLGRAEYGRLGLGENAEEQSEPTPIPDLPKINSVASGA		
	* * : * * * * * * * * : * :		
ggRCC1	SVGYAVSSDGRAFWGMGTNHQLGTGEEEDVWS PVEMTGKQLENRLVLAVSSGGQHTALL		
hRCC1	SVGYAVTKDGRVFAWGMGTNYQLGTGQDEDAWPVEMMGKQLENRVVLSVSSGGQHTVLL		
x1RCC1	SVSYAVSTDGCVFAWGMGTNQLGTGEEEDVWS PEQMTGKHLEDREVLSVSSGGQHTVLL		
	* * . * * * : . * * * . * * * * * * * * : * * . * * * : * * * : * * * : * * * : * * * * * * * * :		
ggRCC1	VKDKARS		
hRCC1	VKDKEQS		
x1RCC1	VRKRS--		
	* . . :		

Supplemental figure 2

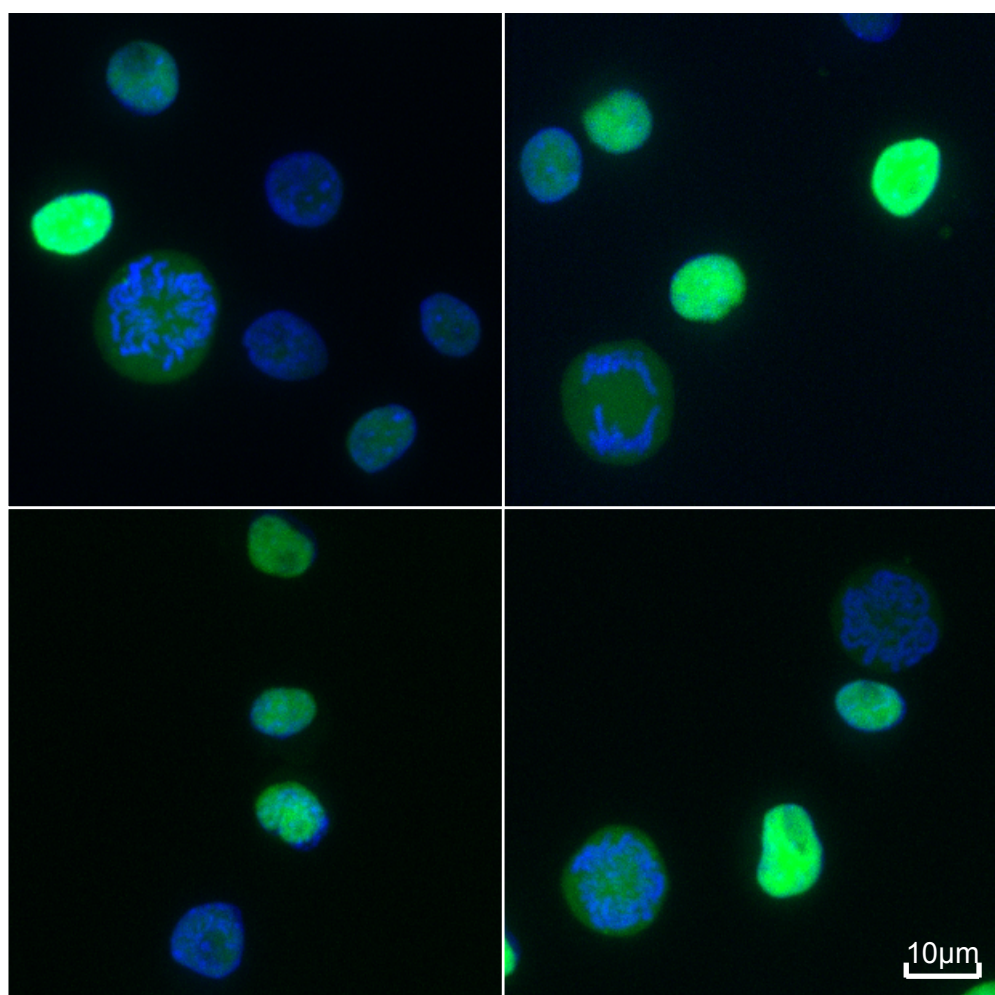


Supplemental figure 3

RCC1^{Δ20}/Histone/DNA



RCC1^{Δ20}/Histone/DNA-NLS



Supplemental figure 4

RCC1	GEF activity	Chromatin binding	Nuclear import	Nuclear localization	Cell viability	Ref.
RCC1 ^{wild}	+	+	+	+	+	
RCC1 ^{Ran}	—	+	+	+	—	Renault et al., 2001
RCC1 ^{Histone/DNA}	+	—	+	+	+	Makde et al., 2010
RCC1 ^{Δ20}	+	+	—	+	+	Renault et al., 1998
RCC1 ^{Δ20/Histone/DNA}	+	—	—	—	—	
RCC1 ^{Δ20/Histone/DNA-NLS}	+	—	+	+	+	

Supplemental figure 5